National Institute of Standards and Technology
Technology Administration, U.S. Department of Commerce

NIST TECHNICAL NOTE 1672

Database-Assisted Design for Wind: Veering Effects on High-Rise Structures

DongHun Yeo and Emil Simiu

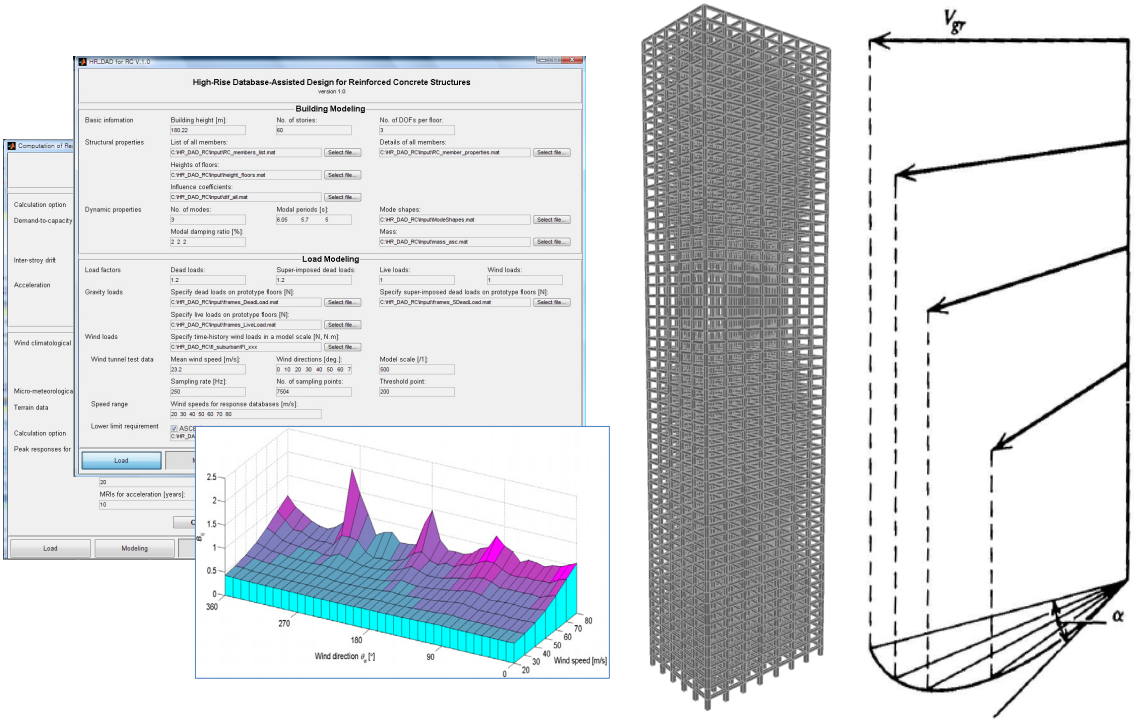

NIST TECHNICAL NOTE 1672

Database-Assisted Design for Wind: Veering Effects on High-Rise Structures

DongHun Yeo and Emil Simiu

Building and Fire Research Laboratory
National Institute of Standards and Technology
Gaithersburg, MD 20899-8611

June 2010

U.S. Department of Commerce
Dr. Gary Locke, *Secretary*

National Institute of Standards and Technology
Dr. Patrick D. Gallagher, *Director*

Disclaimers

(1) The policy of the NIST is to use the International System of Units in its technical communications. In this document however, works of authors outside NIST are cited which describe measurements in certain non-SI units. Thus, it is more practical to include the non-SI unit measurements from these references.

(2) Certain trade names or company products or procedures may be mentioned in the text to specify adequately the experimental procedure or equipment used. In no case does such identification imply recommendation or endorsement by the National Institute of Standards and Technology, nor does it imply that the products or procedures are the best available for the purpose.

Abstract

Atmospheric boundary layer winds experience two types of effects due to friction at the ground surface. One effect is the increase of the wind speeds with height above the surface. The second effect, called the Ekman layer effect, entails veering -- the change of the wind speed direction as a function of height above the surface. In this study a procedure is developed within a database-assisted design (DAD) framework that accounts approximately for veering effects on tall building design.

The procedure was applied in a case study of a 60-story reinforced concrete building, which also considered the dependence of veering effects on the orientation of the building. Comparisons are presented between response estimates that account and do not account for veering. Results show that veering effects on demand-to-capacity indexes for structural members are significant for certain building orientations, and that they increase with the length of the mean recurrence intervals (MRIs). However, for this case study veering effects on inter-story drift and rooftop accelerations were found to be negligible.

Keywords: Building technology; database-assisted design; mean recurrence interval; reinforced concrete; veering.

Acknowledgements

The wind tunnel data used in this report were obtained at the Inter-University Research Centre on Building Aerodynamics and Wind Engineering (CRIACIV-DIC) Boundary Layer Wind Tunnel, Prato, Italy provided by Dr. Ilaria Venanzi of the University of Perugia.

Contents

List of Figures

1. Introduction

Atmospheric boundary layer winds experience two types of effects due to friction at the ground surface. One effect is the increase of the wind speeds with height above the surface. The second effect, called the Ekman layer effect, entails veering -- the change of the wind speed direction as a function of height above the surface. Much research has focused on effects of wind speed profiles, but much research on veering effects on structures are far less documented in the archival literature.

Veering effects of interest for the design of high-rise structures include: (1) effects of continuous wind direction changes with height above ground, and (2) effects due to the difference between the directions of climatological wind speed data at 10 m above terrain with open exposure and of wind speed data at the roof level. Neither type of effect can be studied in typical boundary layer wind tunnels, which do not have the capability to simulate veering.

In this study a procedure is developed within the database-assisted design (DAD) framework that approximately accounts for veering effects on tall building design. A case study is presented in which comparisons are made between structural responses with specified MRIs for buildings with various orientations, obtained by taking and not taking veering effects into account. For that particular case study it is found that, for some building orientations, veering can have significant effects on the design of some members. However, veering effects on inter-story drift and roof-level accelerations were found to be negligible in all cases.

2. Wind direction, veering angle, and building orientation

Veering in the atmospheric boundary layer is associated with the dependence on height of the balance of forces that govern air motion: the pressure gradient force, the Coriolis force, and the friction force, which vanishes at and above the gradient height, and increases from zero at the gradient height to its maximum value at the ground surface. Figure 1 shows that the wind direction in the atmospheric boundary layer describes a spiral, called the *turbulent Ekman spiral*. The angle between the direction of the wind speed at the gradient height and at the surface is defined in meteorological terms as the veering angle. The veering angle is counterclockwise in the northern hemisphere (Figure 2) and clockwise in the southern hemisphere. As represented in Figure 2, the veering angle is 10 ° for open terrain, and 15 ° for densely built suburban terrain at about 500 m elevation (Powell, 2005).

In wind engineering practice, as well as in this report, the veering angle, denoted by α, rather than being defined as in the preceding paragraph, is defined as the difference between the wind direction at the surface of the Earth and the direction at the height of interest. The veering angle so defined is clockwise in the Northern hemisphere and counterclockwise in the Southern hemisphere. As represented in Figure 2, the veering angles at 100 m and 300 m above ground are then about 3 ° and 7 ° over open terrain, respectively, and 5 ° and 10 °, respectively, over densely built suburbs (Powell, 2005); for suburban terrain with roughness intermediate between open and densely built suburban terrain the values of the veering angles may be assumed to be about 4 ° at 100 m and about 8 ° to 9 ° at 300 m. These values, which are tentative, were assumed in the case study presented in this work. Note that according to (Dyrbye and Hansen, 1997), however, the veering angle at higher elevations (i.e., about 1 km) is 20 °, and according to Holmes (2007) it is 30 °.

By convention we consider the North direction as the origin of the angular coordinate β defining wind direction at 10 m above the surface. For example, for wind blowing from the East at 10 m above the surface, β = 90 °. Owing to veering, in the Northern hemisphere wind blowing from direction β at 10 m above the surface will have the direction $\beta + \alpha$ at higher elevations. (In the Southern hemisphere the direction at higher elevations will be $\beta - \alpha$.) For convenience we consider henceforth only wind in the Northern hemisphere.

The orientation of the building is defined by the angle θ_{or} between the North direction and a principal axis of the building denoted by x (Figure 3). The angle between the direction of wind blowing from direction β at 10 m above the surface and a principal axis is then $\beta - \theta_{or}$. Owing to veering, at a higher elevation the angle between that wind and the principal axis x is $\beta - \theta_{or} + \alpha$. For example, let the angle θ_{or} be 30 °. Consider a 300 m tall building with open exposure. For an eastern wind (wind blowing from direction β = 90 ° at 10 m above the surface) the angle between that direction and the principal axis x is 90 ° - 30 ° = 60 ° at 10 m above the surface. Owing to veering the direction of the eastern wind changes at higher elevations. At the top of the building the direction of the wind blowing from the East at 10 m above the Earth's surface will be 97 ° with respect to the North direction, and the angle θ_w between that direction and the x axis of the building will be 97 ° - 30 ° = 67 °.

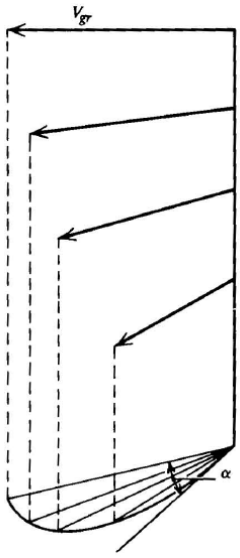

Figure 1. Wind velocity directions in the atmospheric boundary layer, wind engineering convention (Simiu and Scanlan, 1996)

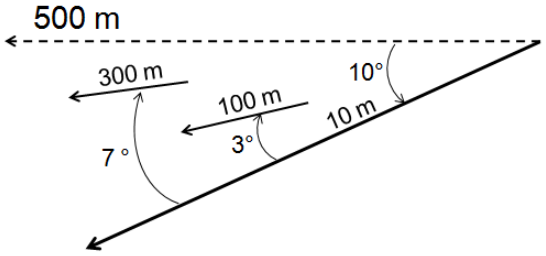

(a) Open terrain

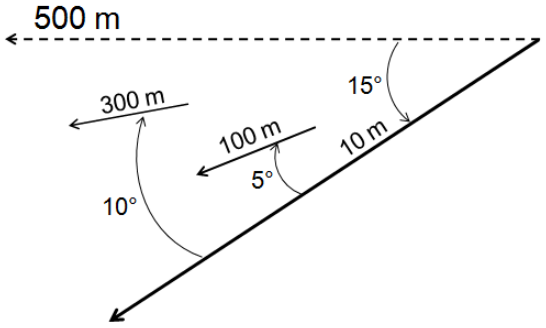

(b) Densely built suburban terrain

Figure 2. Suggested values of veering angles (Powell 2005)

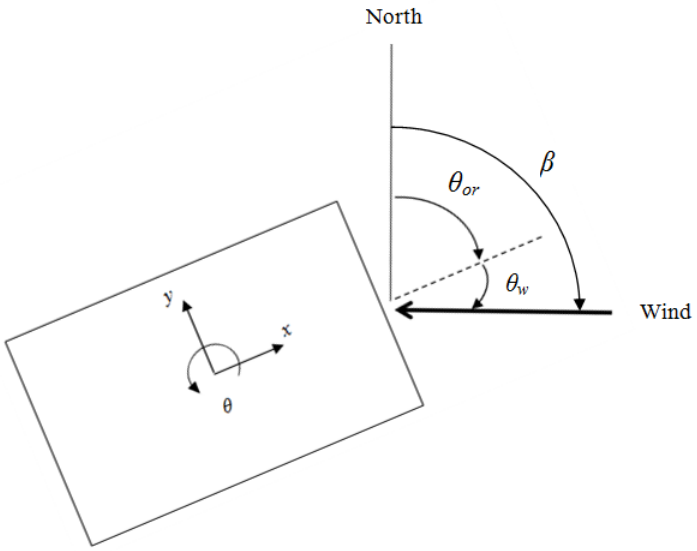

Figure 3. Angles defining building orientation and wind direction at 10 m above the Earth's surface

3. Procedure for estimating veering effects on building response

The effects of veering are estimated by calculating the response in two ways. First, the response of the structure subjected to wind loads is calculated by disregarding veering. Second, the response is calculated by taking veering into account. Because wind tunnels typically do not simulate veering, it is necessary in calculations to resort to a simplified model of veering. In this model the veering angle is constant over the entire building height and is equal to the assumed veering angle at the top of the building. This model typically results in conservative estimates of veering effects on the building response.

In this work veering effects are studied within the framework of the database-assisted design (DAD) technique, which requires the following wind engineering input: (1) an aerodynamic database of the pressure coefficient time histories at a sufficiently large number of taps on the building model envelope, (2) a local climatological database of wind speeds at the standard elevation (typically 10 m above ground over open terrain), and (3) a micro-meteorological data set consisting of ratios between mean hourly wind speeds at the elevation of the building rooftop on the one hand and the corresponding directional 3-s or 10-min wind speed at the standard elevation of the meteorological site. Once the wind engineering input is available, the response calculations can be performed by using the High-Rise Database-Assisted Design for Reinforced Concrete Structures (HR_DAD_RC) software. The procedure on which the software is based is now described. For details see Yeo (2010).

1. A time series of pressure coefficients are used to produce the time series of (a) horizontal wind force components along the principal axes of the building, applied at the center of mass of each floor or group of floors, and (b) torsional moments about those centers of mass. This task is performed separately for each wind direction, and for wind speeds blowing from that direction of, say, 20 m/s, 30 m/s,…, 80 m/s. The outputs of this task are time series of wind loads induced by winds with those speeds, for every wind direction being considered (e.g., 0˚, 10˚,…, 350˚, or 0˚, 22.5˚,…, 337.5˚). Note that this task is independent of the wind climate at or near the building site, and that the output just mentioned is an aerodynamic property of the building.

2. A dynamic analysis of the building is performed for each wind speed and direction listed in item 1 above. This analysis yields the respective time histories of the inertial forces and torsional moments acting at and around the centers of mass of the floors or groups of floors being considered. The sums of the applied wind loads and of the inertial loads represent the total wind-induced loads acting on the structure.

3. Once the total horizontal wind loads are available, HR_DAD produces time series of the wind effects of concern by multiplying the total loads by the appropriate influence coefficients. The wind effects being calculated should be those that are of direct concern to the designer. The member design is checked using (a) interaction equations of internal forces due to wind effects and gravity loads and (b) the section capacity. (These are referred to as demand-to-capacity indexes (DCIs), and typically consist of demand-to-capacity ratios.) Additional wind effects of concern are inter-story drift and top floor accelerations. Note that all the wind effects are calcu-

lated for each of the wind directions and for each of the wind speeds listed in item 1 above. This task is performed automatically by the HR_DAD software. Its output consists of *wind effect databases* (also referred to as *response databases*) representing the wind effects being sought as a function of wind direction and wind speed. This output is also a property of the structure, independent of wind climate at or near the site. In a response database the wind directions are referenced with respect to a principal axis of the building. For an example see Figure 4.

4. The wind effect databases enable the conversion of the $m \times n$ matrix, whose elements are directional wind speeds v_{ij} (m is the number of windstorm events or years of record and n is the number of wind directions; $i = 1, 2, ..., m$; $j = 1, 2,\ldots, n$), into a matrix with the same dimensions whose elements are wind effects (e.g., individual member DCIs, inter-story drift, and top floor accelerations) induced by the directional wind speeds v_{ij}. Denote the elements of this matrix by r_{ij}. For each row of the matrix whose elements are r_{ij}, only the wind effect $\max_j(r_{ij})$ is of interest from a structural design viewpoint and is therefore retained. The requisite operations are performed automatically by the HR_DAD software, giving rise to the vector $\max_j(r_{ij})$. That vector is rank-ordered, and given the arrival rate of the wind storm events, each of its m rank-ordered components corresponds to an MRI automatically calculated by the HR_DAD software.

Veering effects are taken into account in item 4 above. Two wind effects are estimated assuming: (1) no veering, and (2) uniform veering. For the no veering case, the response database is rotated clockwise by the angle of building orientation θ_{or}; owing to this rotation, the wind directions considered in the response database are referenced with respect to the same angular origin (i.e., the North direction) as the wind directions at 10 m above ground, rather than with respect to the principal axis x of the building. For the uniform veering case, the response database is rotated clockwise by the angle $\theta_{or} + \alpha$. The wind effects of interest based on assumptions (1) and (2) above are used for veering effects estimation. Note that for the response database and the wind climatological database used in the HR_DAD calculations the reference height of all winds is the top of the building, just as it is for the aerodynamic database obtained in the wind tunnel. Note that the estimation of veering effects is dependent on resolution of the directional wind datasets being used, which in this study is 22.5°. A wind climatological database with a higher resolution will estimate the veering effects more accurately.

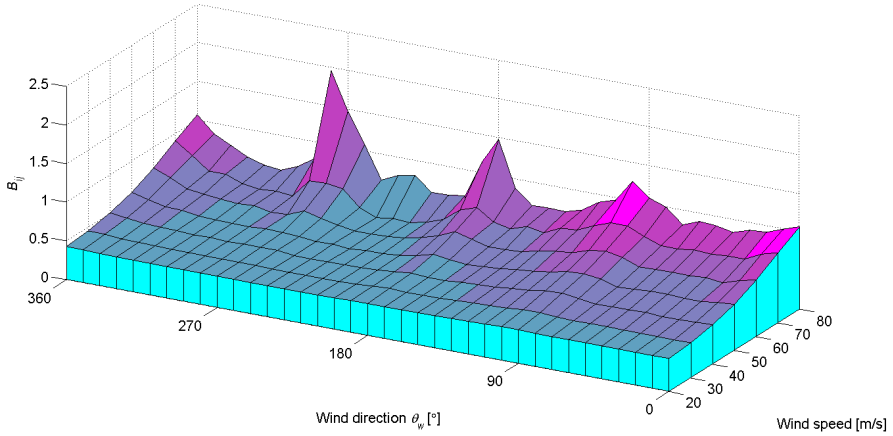

Figure 4. Example of a wind effects database. The wind effects consist for this plot of a set of demand-to-capacity index B_{ij} for a tall building column.

4. Structural response

The loads induce in the structure three types of response of interest in design: demand-to capacity indexes (Sect. 4.1), inter-story drift (Sect. 4.2), and accelerations at the top floor (Sect. 4.3). For details see Yeo (2010).

4.1 *Demand-to-capacity indexes*

The demand-to-capacity index is a quantity used to measure the adequacy of a structural member from the point of view of strength. In general, this index is defined as a sum of ratios of internal forces induced by the design loads at a member cross section to the strength available at that cross section. The design strength in HR_DAD_RC is based on the Building Code Requirements for Structural Concrete and Commentary 318-08 (hereinafter ACI 318-08). An index higher than unity indicates that the design of a structural member is inadequate. The HR_DAD_RC software employs two demand-to-capacity indexes: one for axial or/and flexural loads, and one for shear and torsion.

The index "B_{ij}^{PM}" pertains to the axial load and bending moment for columns, and to and bending moments for beams. Depending upon whether the section is controlled by tension or compression, the index has the form

$$\begin{aligned} B_{ij}^{PM} &= \frac{M_u}{\phi_m M_n} && \text{(for a tension-controlled section)} \\ &= \frac{P_u}{\phi_p P_n} && \text{(for a compression-controlled section)} \end{aligned} \tag{1}$$

where M_u and P_u are the bending moment and axial force at the section being considered, M_n and P_n are the nominal moment and axial strengths at that section, and ϕ_m and ϕ_p are the capacity reduction factors for flexural and axial strengths, respectively. In particular, for columns subject to bi-axial flexure loads, the Bresler reciprocal load method of R10.3.6 in ACI 318-08 (2008) is used for compression-controlled sections, and the PCA (Portland Cement Association) load contour method (PCA, 2008) is used for tension-controlled sections; these methods involve sums of terms similar to those of Eq. (1).

The index "B_{ij}^{VT}" is associated with interaction equation for shear forces and torsional moment for columns and beams:

$$B_{ij}^{VT} = \frac{\sqrt{V_u^{\,2} + \left(\dfrac{T_u p_h b_w d}{1.7 A_{oh}^{\,2}} \right)^2}}{\phi_v \left(V_c + V_s \right)} \tag{2}$$

where V_c and V_s are the nominal shear strengths provided by the concrete and the reinforcement, respectively, V_u is the shear force, T_u is the torsional moment, ϕ_v is the reduction factor for shear strength, p_h is the perimeter enclosed by the centerline of the outermost closed stirrups, A_{oh}

is the area enclosed by the centerline of the outermost closed stirrups, b_w is the width of the member, and d is the distance from the extreme compression fiber to the centroid of longitudinal tension reinforcement.

4.2 *Inter-story drift*

The time series of inter-story drifts at the i^{th} story, $d_{i,x}(t)$ and $d_{i,y}(t)$ (Figure 5) corresponding to the x and y axes, respectively, are:

$$d_{i,x}(t) = \frac{\left[x_i(t) - D_{i,y}\theta_i(t)\right] - \left[x_{i-1}(t) - D_{i-1,y}\theta_{i-1}(t)\right]}{h_i}$$
$$d_{i,y}(t) = \frac{\left[y_i(t) + D_{i,x}\theta_i(t)\right] - \left[y_{i-1}(t) + D_{i-1,x}\theta_{i-1}(t)\right]}{h_i} \quad (3)$$

where $x_i(t)$, $y_i(t)$, and $\theta_i(t)$ are the displacements of and the rotation about the mass center at the i^{th} floor, $D_{i,x}$ and $D_{i,y}$ are distances along the x and y axes from the mass center on the i^{th} floor to the point of interest on that floor, and h_i is the i^{th} story height (i.e., the vertical distance between the mass centers of the i^{th} and the $(i\text{-}1)^{th}$ floor).

The ASCE 7-05 Commentary (2005) suggests limits on the order of 1/600 to 1/400 for an annual probability of exceedance of 0.05, i.e., for a mean recurrence interval (MRI) of 20 years (see Section CC.1.2 in ASCE 7-05).

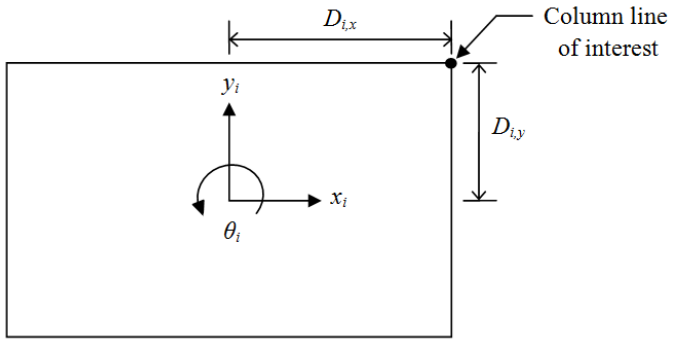

Figure 5. Position parameters at floor i for inter-story drift

4.3 *Top floor acceleration*

The time series of the resultant acceleration at the top floor, $a_r(t)$ is obtained in HR_DAD_RC by the expression:

$$a_r(t) = \sqrt{\left[\ddot{x}_{top}(t) - D_{top,y}\ddot{\theta}_{top}(t)\right]^2 + \left[\ddot{y}_{top}(t) + D_{top,x}\ddot{\theta}_{top}(t)\right]^2} \quad (4)$$

where the accelerations $\ddot{x}_{top}(t)$, $\ddot{y}_{top}(t)$, and $\ddot{\theta}_{top}(t)$ of the mass center at the top floor pertain to the x, y, and θ (i.e., rotational) axes, and $D_{top,x}$ and $D_{top,y}$ are the distances along the x and y axes from the mass center to the point of interest on the top floor.

The resultant value in Eq. (4) is used, instead of accelerations along the principal axes, because the peak acceleration is of concern regardless of its direction. ASCE 7-05 does not provide wind-related peak acceleration limits. However, for office buildings, a limit of 25 mg_n (i.e., milli-gravity acceleration) for a 10 year MRI was suggested by Isyumov et al. (1992) and Kareem (1999) where mg_n is the milli-gravity acceleration.

5. Case study and results

A 60-story reinforced concrete building with rigid diaphragm floors was designed using the software High-Rise Database-Assisted Design for Reinforced Concrete structures (HR_DAD_RC) developed by NIST (Yeo, 2010). The building, known as the Commonwealth Advisory Aeronautical Research Council (CAARC) building, has dimensions 45.72 m in width, 30.48 m in depth, and 182.88 m in height. It has a moment-resistant frame structural system consisting of 2880 columns and 4920 beams, and is similar to the structural system studied by Teshigawara (2001). The building was assumed to be located near Miami, Florida and have suburban exposure. For details see (Yeo, 2010).

Time histories of aerodynamic wind loads on each floor were calculated from time series of pressure coefficients on a rigid wind tunnel model of the CAARC building. The aerodynamic data were obtained at the Inter-University Research Center on Building Aerodynamics and Wind Engineering (CRIACIV-DIC) Boundary Layer Wind Tunnel in Prato, Italy (Venanzi, 2005). The loads for 36 wind directions (10 ° increments) were obtained from directional pressure data measured from taps on the envelope of the building. Figure 6 shows a typical set of four structural members selected for the calculation of wind effects. For demand-to-capacity indexes structural members were chosen as follows: a corner column (cc), a non-corner column (cn), an exterior beam (be), and an interior beam (bi). Mean recurrence intervals (MRIs) of 300, 700, and 1700 years were considered. The indexes for MRI = 300 years are not appropriate in a 60 story building; however, they were employed in this study for comparisons with results obtained for higher MRIs.

The climatological database used in the study is a wind speed dataset of 999 simulated hurricanes for 16 directions near Miami (Milepost 1450), obtained from the site www.nist.gov/wind (Batts et al., 1980). The angles indicating those directions (β) are from 22.5° to 360° clockwise from the North in 22.5° increments. Other hurricane wind speeds data sets are available commercially.

Because the wind climatological database corresponds to open exposure in all directions, the veering angle is estimated to be 5 ° from 10 m to the building roof elevation (i.e., 182.88 m) by linear interpolation from Figure 2. For each of the 999 storm events only the largest of the 16 directional responses is of interest and was retained. This yielded a vector of the 999 largest directional responses. The peak response database, consisting of the vector of those 999 values, allows the estimation of the peak response corresponding to specified MRIs through the use of the non-parametric estimation method described in of Simiu and Miyata (2006), Sect. 2.4.3.2.2. Note that the MRIs pertain to load effects, not to wind loads.

Figure 7 shows peak response databases for demand-to-capacity indexes of the corner column (cc) for the building orientation θ_{or} = 90 °. Differences between indexes corresponding to the no veering and uniform veering cases are negligible for low MRIs, but are modestly significant for high MRIs.

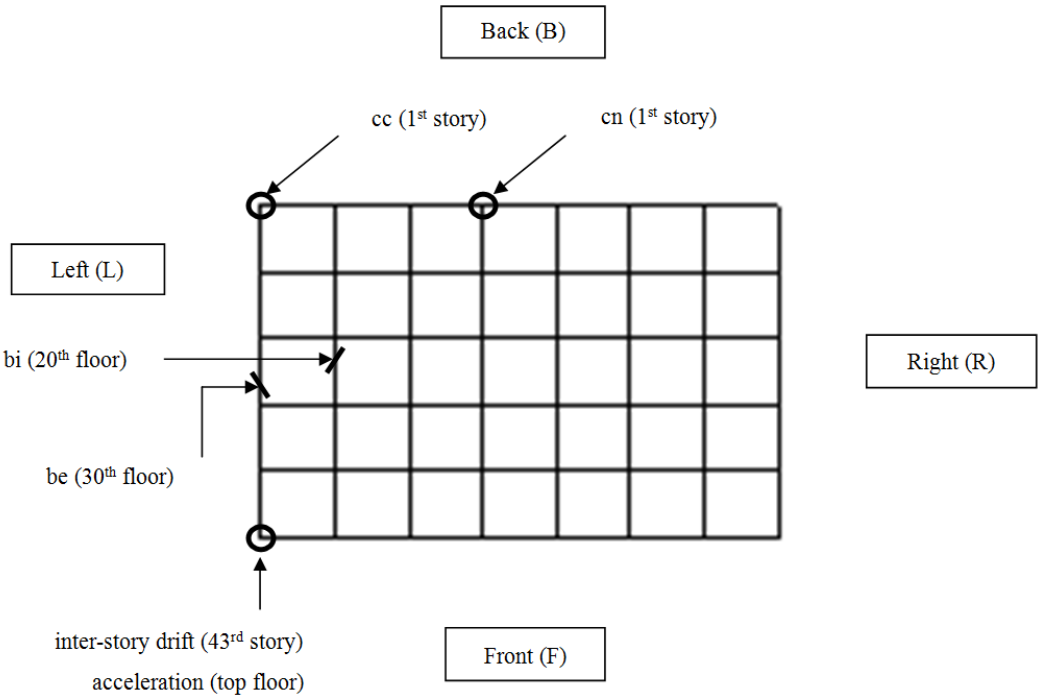

Figure 6. Plan view of building with locations of selected members ($\theta_{or} = 90°$)
(cc = corner column; cn = internal column; be = exterior beam; bi = interior beam)

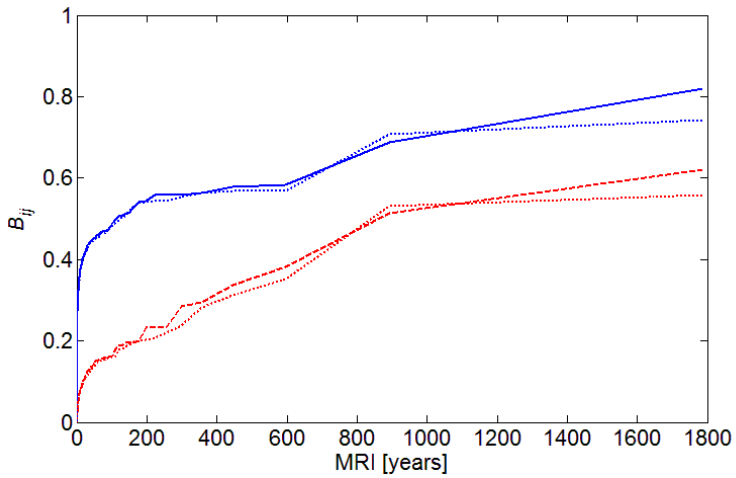

Figure 7. Demand-to-capacity indexes as functions of MRIs for building orientation ($\theta_{or} = 90°$)
(for no veering, B_{ij}^{PM} ·····, B_{ij}^{VT} ·····; for uniform veering, B_{ij}^{PM} ——, B_{ij}^{VT} - - - -)

Effects of veering as functions of building orientation were also investigated. Peak demand-to-capacity indexes are shown as functions of building orientation in Figures 8 and 9 for two cases: (1) no veering and (2) uniform veering.

For B_{ij}^{PM} veering effects on both columns and beams are stronger for higher MRIs. This is due to the strong directional dependence of the responses for high wind speeds. For the corner column the veering effects are very small for MRI = 300 years but increase up to approximately 20 % for MRI = 1700 years. The veering effects significantly depend on building orientation, and their variation with building orientation also become larger as MRI increases. The B_{ij}^{PM} indexes for the 1700 year MRI vary as functions of building orientation from 0.73 to 0.93 for the corner column, 0.74 to 0.84 for the non-corner column, 0.50 to 0.66 for the exterior beam, and 0.55 to 0.73 for the interior beam.

For B_{ij}^{VT} the indexes for MRI = 1700 years increase by approximately 30 % and 10 % owing to uniform veering for columns and beams, respectively; the veering effects also show significant dependence on building orientation. In particular, this dependence is high even for MRI = 300 years for the corner column. For both corner and non-corner columns the index increases by more than 100 % at MRI = 1700 years.

The results show that veering effects for the columns are much larger for B_{ij}^{VT} than for B_{ij}^{PM}. Veering effects for beams exhibit smaller increases with MRIs, and change with building orientation less, than veering effects for columns.

Figure 10 shows demand-to-capacity indexes based on (a) estimates of veering effects and (b) no veering effects, for 300 year and 1700 year MRI, respectively. For a given building orientation, if the index accounting for veering effects is equal to or less than the index estimated without accounting for the veering effects, the effect of veering is disregarded.

Inter-story drift was calculated for a 20 year MRI, along the principal axes (i.e., *x* and *y*) and as a resultant of the *x* and *y* components, for the front-left corner of the 43rd story (Figure 6). Veering effects were found to be about 3 % or less. The variation of veering effects with building orientation was also found to be small (less than 10 %).

Peak top floor acceleration for a 10 year MRI was estimated for the front-left corner along the *x*-axis defining building orientation (Figure 6). Acceleration increases due to veering do not exceed 5 %, and do not exhibit significant directionality preference due to building orientation.

The results show that serviceability design can ignore veering effects because these responses have low sensitivity to wind direction at MRIs of the order of, say, 20 years.

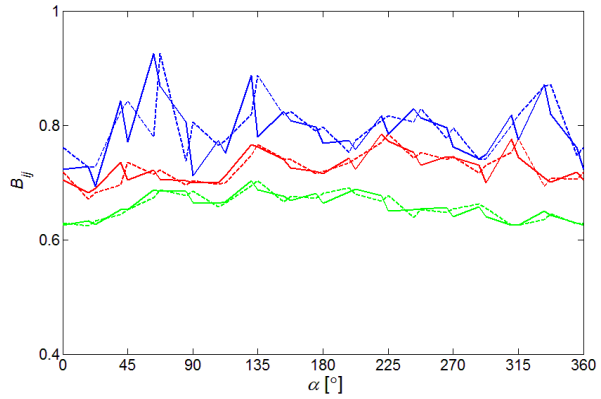

(a) Corner column (cc)

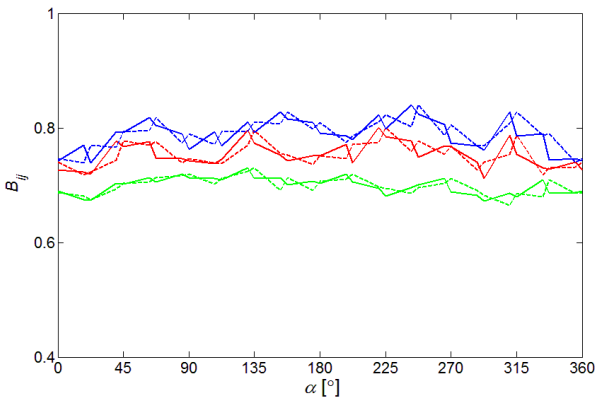

(b) Non-corner column (cn)

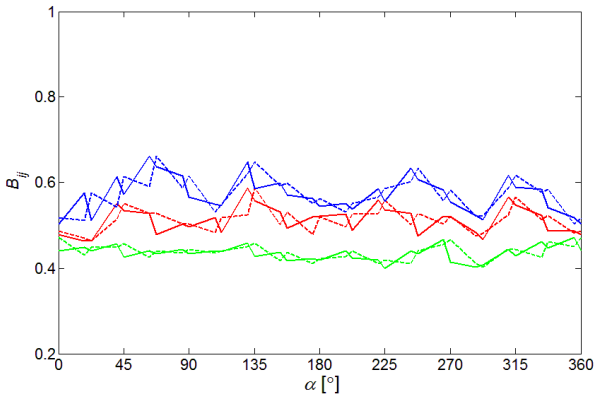

(c) Exterior beam (be)

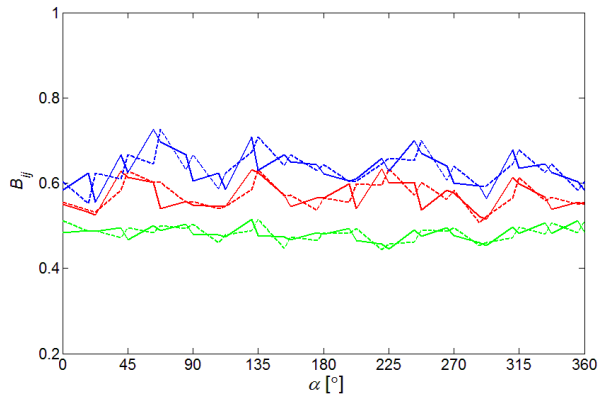

(d) Interior beam (bi)

Figure 8. Peak demand-to-capacity indexes (B_{ij}^{PM})

(for MRI = 300 years, - - - no veering, ——— uniform veering;
for MRI = 700 years, - - - no veering, ——— uniform veering;
for MRI = 1700 years, - - - no veering, ——— uniform veering)

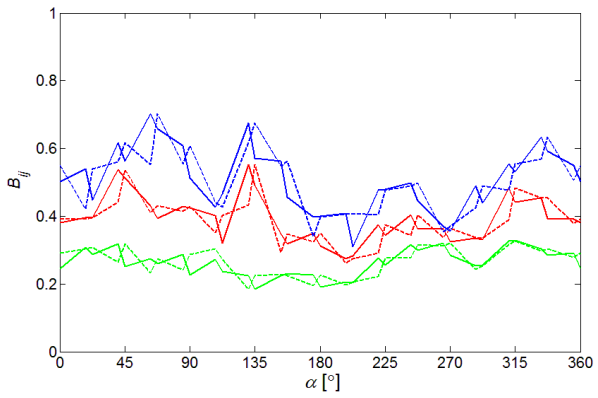

(a) Corner column (cc)

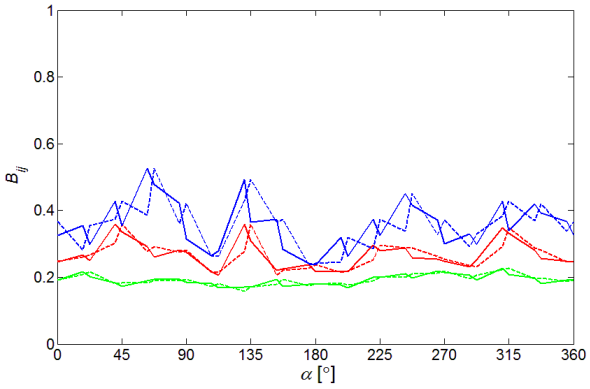

(b) Non-corner column (cn)

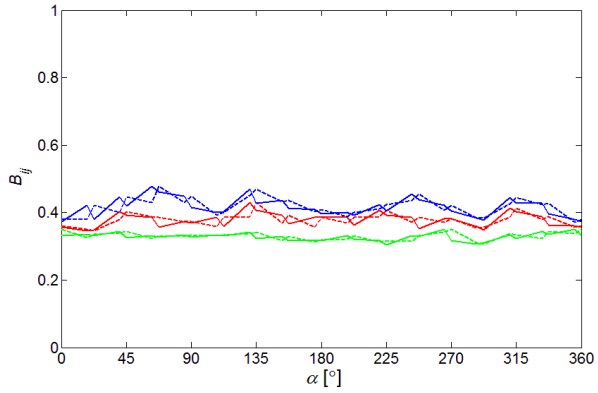

(c) Exterior beam (be)

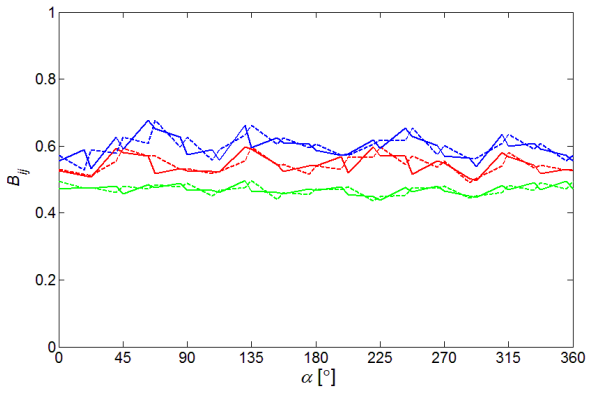

(d) Interior beam (bi)

Figure 9. Peak demand-to-capacity indexes (B_{ij}^{VT})

(for MRI = 300 years, – – – no veering, ——— uniform veering;
for MRI = 700 years, – – – no veering, ——— uniform veering;
for MRI = 1700 years, – – – no veering, ——— uniform veering)

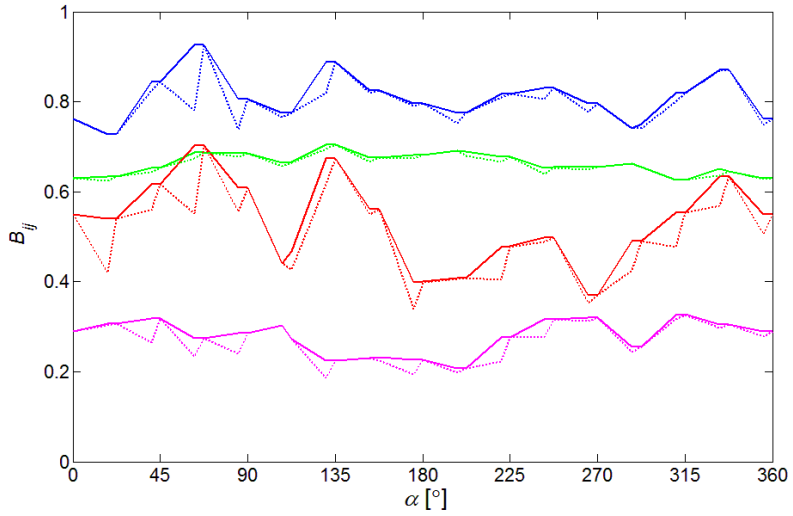

(a) Corner column (cc)

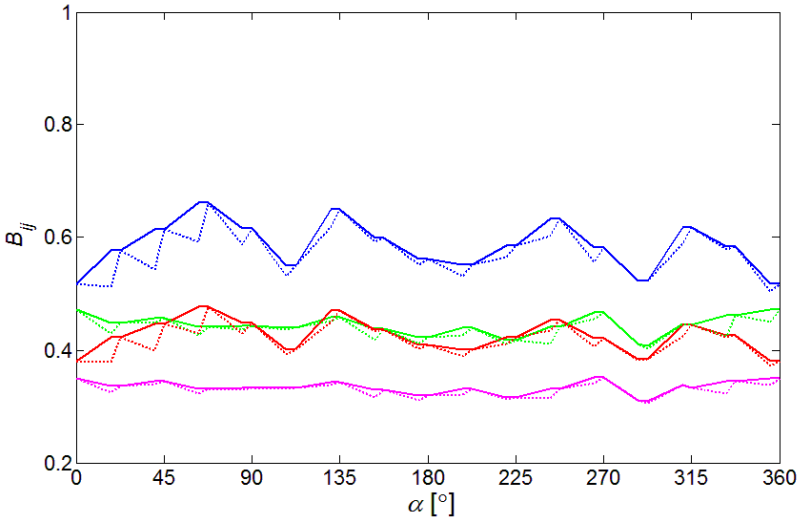

(b) Exterior beam (be)

Figure 10. Demand-to-capacity indexes with or without veering effects

(for B_{ij}^{PM} with veering effects, MRI = 300 years, MRI = 1700 years;
for B_{ij}^{PM} without veering effects, MRI = 300 years, MRI = 1700 years;
for B_{ij}^{VT} with veering effects, MRI = 300 years, MRI =1700 years;
for B_{ij}^{VT} without veering effects, MRI = 300 years, MRI =1700 years)

6. Conclusions

This study suggests an approach to estimation of veering effects estimated by comparing responses under the assumptions of (1) no veering and (2) uniform veering over the entire building height equal to the veering at the roof of the building. The analysis for veering effects was conducted for a specific design of the CAARC building in a specific area, Miami, in suburban terrain exposure. The estimates of the veering effects are typically conservative, owing to the assumption of a uniform veering angle throughout the building height.

According to the results obtained for this case study, veering effects on demand-to-capacity indexes used for the strength design of structural members increase with mean recurrence interval (MRI). The veering effects for columns were much larger for the shear/torsion demand-to-capacity index B_{ij}^{VT} than for its axial force/moment counterpart B_{ij}^{PM}. The veering effects also significantly depend on building orientation, particularly for higher MRIs. The results indicate that the design of structural members designed for high MRIs (e.g., 1700 years) should account for veering effects if the structural responses are significantly dependent on wind direction.

Inter-story drift and top floor acceleration, however, exhibited negligible veering effects, and their dependence on building orientation is weak.

The conclusions based on this application would clearly differ for different types of building or conditions. Software for implementing the DAD procedure used in this study is available on www.nist.gov/wind. To the authors' knowledge this is the first study that quantifies effects of veering on high-rise buildings by using a documented estimation method available in the public domain.

References

ACI. 2008. Building code requirements for structural concrete (ACI 318-08) and commentary. American Concrete Institute, Farmington Hills, MI.
ASCE. 2005. Minimum design loads for buildings and other structures. ASCE Standard ASCE/SEI 7-05, American Society of Civil Engineers, Reston, VA.
Batts, M.E., Russell, L.R., Simiu, E., 1980. Hurricane wind speeds in the United States. Journal of the Structural Division-ASCE 106(10), 2001-2016.
Dyrbye, C., Hansen, S.O., 1997. Wind loads on structures. John Wiley & Sons.
Holmes, J.D., 2007. Wind loading of structures. Spon Press, New York.
Isyumov, N., Fediw, A.A., Colaco, J., Banavalkar, P.V., 1992. Performance of a tall building under wind action. Journal of Wind Engineering and Industrial Aerodynamics 42(1-3), 1053-1064.
Kareem, A., Kijewski, T., Tamura, Y., 1999. Mitigation of motions of tall buildings with specific examples of recent applications. Wind and Structures 2(3), 201-251.
PCA, 2008. PCA notes on 318-08 building code requirements for structural concrete with design applications. Portland Cement Association, Skokie, IL.
Powell, M.D. 2005. pesonal communication.
Simiu, E., Miyata, T., 2006. Design of buildings and bridges for wind: a practical guide for ASCE-7 Standard users and designers of special structures. John Wiley & Sons, Hoboken, NJ.
Simiu, E., Scanlan, R.H., 1996. Wind effects on structures. John Wiley & Sons.
Teshigawara, M., 2001. Structural design principles (chapter 6), in: Design of modern highrise reinforced concrete structures, H. Aoyama, ed., Imperial College Press, London.
Venanzi, I., 2005. Analysis of the torsional response of wind-excited high-rise building. Ph.D. Dissertation, Università degli Studi di Perugia.
Yeo, D., 2010. Database-Assisted Design of high-rise reinforced concrete structures for wind: Concepts, software, and application. NIST Technical Note 1665, National Institute of Standards and Technology, Gaithersburg, MD.